Energy loss rate for guiding-center antihydrogen atoms

Eric M. Bass and Daniel H. E. Dubin
Department of Physics, University of California, San Diego, La Jolla, California 92093

(Received 22 October 2003; accepted 12 December 2003)

Collisional drag between a bound positron and a background positron plasma is considered as a mechanism for guiding-center antihydrogen atoms to relax to deeply bound states. Contrary to previous assessment, an adiabatic cutoff to the drag is predicted at deep binding, when the bound positron's **E×B** drift speed v_d exceeds the plasma positron thermal speed. In this regime, small-impact parameter collisions neglected in the drag calculation become the dominant 3-body recombination mechanism. At shallow binding, when $\xi = v_d/\overline{v} \ll 1$, the atom's energy loss rate due to drag scales like $\xi^{3/2}\log^2\xi$. When $\xi \gg 1$ the adiabatic cutoff takes over and the rate scales as $\xi^{7/6}\exp(-\frac{3}{2}(2\xi)^{2/3})$. The adiabatic cutoff implies that collisional drag can only assist positron–antiproton recombination up to a finite binding energy.
[DOI: 10.1063/1.1646392]

Current attempts to produce antihydrogen[1,2] employ nested Penning traps to immerse antiprotons in a cold positron plasma. At the cryogenic temperatures used in the experiments, the plasma is in the regime of strong magnetization, where the dimensionless parameter $\chi \equiv \overline{v}/\Omega_c b = r_c/b \ll 1$. Here, $\overline{v}$, Ω_c, and r_c are the positron thermal speed, cyclotron frequency, and cyclotron radius, respectively, and $b = e^2/k_B T$ is the distance of closest approach. In this regime, three-body recombination is predicted to be the rate-limiting recombination mechanism. The recombination rate R_3 is dominated by a kinetic bottleneck at binding energies U of order $4k_BT$.[3] At this weak binding energy, the positron–antiproton pair form a "guiding-center atom," where the positron **E×B** drifts around the antiproton at a distance r of order b, and oscillates along the magnetic field in the antiproton's potential well (Fig. 1). Assuming for simplicity that the antiproton is stationary, O'Neil and Glinsky calculated that $R_3 = 0.07n^2\overline{v}b^5$, where n is the plasma positron density. The drift orbit frequency $\omega \approx ec/Br^3$ for small parallel bounce motion and is slower than oscillations parallel to the field.

Here, we consider a different rate: the energy loss rate γ. The above-quoted theoretical rate R_3 is actually the rate at which atoms form with binding energies greater than $4k_BT$. Beyond this bottleneck, atoms have a good chance of eventually falling to the ground state without being reionized. However, $4k_BT$ is still relatively shallow binding. The energy loss rate γ is the average rate at which guiding-center atoms move to deeper binding *once they are past the bottleneck*. This rate is of interest because in current experiments, various effects limit the time available to the atoms to completely recombine to the ground state: for example, atoms can drift out of the plasma where they may encounter strong electric fields that reionize them unless they are deeply bound.

The energy loss due to three-body collisions is due to two processes: close collisions with impact parameters ρ less than the atom size r, and distant collisions with $\rho > r$. Each process has been considered previously. In Ref. 3, the close collisions with $\rho < r$ were shown to produce an energy loss rate that scales as

$$\gamma_{\text{close}} \approx \frac{n\overline{v}b^2}{\epsilon^2}, \tag{1}$$

where $\epsilon = U/k_BT$ is the scaled binding energy. This rate clearly decreases as the atom falls to tight binding because the cross section for close collisions is reduced as the atom becomes smaller.

The energy loss rate due to distant collisions with $\rho > r$ was considered by Men'shikov and Fedichev,[4,5] and it is this work which we re-examine here. These authors found that distant collisions create a drag force on the bound positron that causes it to move to deeper binding. Furthermore, they observed that the more tightly bound the positron, the faster it moves, and the larger the drag force, leading to an energy loss rate that monotonically increases with binding energy, eventually dominating over the rate due to close collisions.

However, these authors neglected the effect of the bound positron's **E×B** drift motion on the collisional drag coefficient. Here, we show that when this motion is included, an adiabatic cutoff of the drag force is encountered at tight binding. When the drift speed of the bound positron becomes larger than the plasma positron thermal speed, the plasma positrons can no longer respond to the bound positron's rotational **E×B** drift motion. As a result, we find that collisional drag due to distant collisions is no longer important at deep binding, but can play an important role at shallow binding energies, depending on the specific parameters of the experiment (i.e., the value of χ, which depends on plasma temperature and magnetic field strength). In particular, we find that the adiabatic cutoff occurs for scaled energies ϵ near

$$\epsilon_{\text{cutoff}} = \sqrt{\frac{1}{\chi}} = \sqrt{\frac{b}{r_c}}.$$

Plasma positrons streaming past the atom along the magnetic field impart random kicks to the bound positron and give it diffusive mobility in the potential well of the antipro-

1070-664X/2004/11(3)/1240/4/$22.00

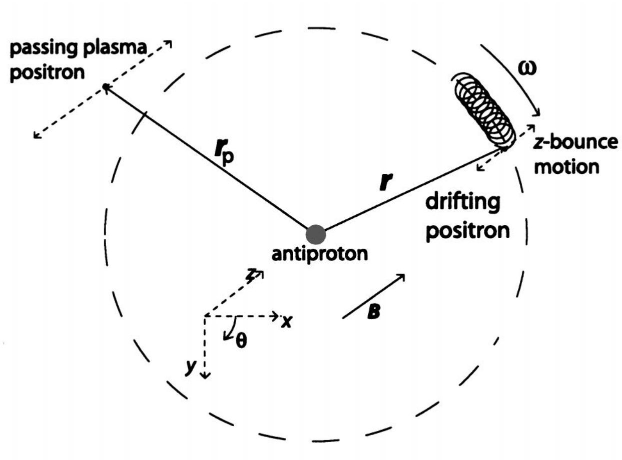

FIG. 1. A guiding center atom. The positron **E×B** drifts in the electric field of a stationary antiproton while oscillating back and forth along the magnetic field in the potential well of the antiproton. The drift orbit frequency $\omega \approx ec/Br^3$ for small bounce motion and is slower than oscillations parallel to the field.

ton. If the diffusion tensor **D** is known, then the ensemble averaged flux Γ of positrons bound in a potential field ϕ is given by the Einstein relation[6]

$$\mathbf{\Gamma} \equiv \mathbf{\Gamma}_d + \mathbf{\Gamma}_m = -\mathbf{D} \cdot \left(\nabla n + \frac{en}{k_B T} \nabla \phi \right).$$

The mobility flux $\mathbf{\Gamma}_m$ to lower binding energy is given by the second term. Thus, a single positron will, on average, move to deeper binding with velocity

$$\mathbf{v} = \frac{\mathbf{\Gamma}_m}{n} = -\mathbf{D} \cdot \frac{e}{k_B T} \nabla \phi.$$

Let us assume cylindrical coordinates centered on the antiproton with the magnetic field oriented along $\hat{\mathbf{z}}$, the unit vector in the z direction (Fig. 1). For simplicity, we neglect the bound positron's bounce motion along the magnetic field and consider only the cross field drift motion. In this limit, binding energy takes the point particle form

$$U = \frac{e^2}{r}.$$

(Note that the positron's perpendicular kinetic energy is neglected in the guiding-center approximation.) Since we expect the diffusion tensor to be diagonal in cylindrical coordinates, we can let D_r be the diffusion coefficient in the radial direction. Because $\hat{\mathbf{r}}$ is parallel to $\nabla \phi$, D_r represents the positron's mobility in the background potential well of the antiproton. The change in binding energy U is given by

$$\frac{\partial U}{\partial t} = -e\mathbf{v} \cdot \nabla \phi = \frac{D_r e^2}{k_B T} (\nabla \phi)^2. \tag{2}$$

Recalling that the positron **E×B** drifts in the potential field ϕ, we can use

$$\mathbf{v}_d = \frac{c}{B} \hat{\mathbf{z}} \times \nabla \phi$$

to rewrite Eq. (2) in terms of the drift velocity magnitude v_d,

$$\frac{\partial U}{\partial t} = \frac{D_r e^2}{k_B T} \left(\frac{v_d B}{c} \right)^2.$$

The energy loss rate due to drag, γ_{drag}, is

$$\gamma_{\text{drag}} \equiv \frac{1}{U} \frac{\partial U}{\partial t} = \frac{r D_r}{k_B T} \left(\frac{v_d B}{c} \right)^2. \tag{3}$$

With a known diffusion coefficient and drift velocity, Eq. (3) gives us the rate at which a bound positron moves to deeper binding. The diffusion coefficient depends on relative motion between plasma positrons and the bound positron. The adiabatic cutoff mentioned above manifests through this diffusion coefficient.

To calculate the diffusion coefficient, we employ the collisional definition

$$D_r = \tfrac{1}{2} \langle \nu \Delta r^2 \rangle, \tag{4}$$

where ν is the frequency of collisions between the bound positron and passing plasma positrons and Δr is the displacement along r experienced during each collision. Consider a guiding-center atom immersed in a magnetized positron plasma. The bound positron orbits the antiproton with frequency $\omega = v_d / r$. To first order, plasma positrons are confined to move along magnetic field lines at a constant velocity v_z. As each plasma positron travels by the atom, its electric field perturbs the drift velocity of the bound positron by

$$\mathbf{v}_1(t) = \frac{ce}{B} \frac{(\mathbf{r}(t) - \mathbf{r}_p(t)) \times \hat{\mathbf{z}}}{|\mathbf{r}(t) - \mathbf{r}_p(t)|^3}.$$

Here $\mathbf{r}(t)$ is the position of the bound positron, and $\mathbf{r}_p(t)$ is the position of the passing plasma positron (Fig. 1). Without loss of generality, we can let the passing positron pass through the $z=0$ plane at $t=0$ when the bound positron is at $\theta=0$ in its orbital cycle. We therefore write

$$\mathbf{r}(t) = r(\cos \omega t \hat{\mathbf{x}} + \sin \omega t \hat{\mathbf{y}}),$$

$$\mathbf{r}_p(t) = x_p \hat{\mathbf{x}} + y_p \hat{\mathbf{y}} + v_z t \hat{\mathbf{z}}.$$

If $r_p \gg r$, the radial component of the bound positron's velocity perturbation is

$$v_r = \mathbf{v}_1 \cdot \hat{\mathbf{r}} = \frac{ce}{B} \frac{(x_p \sin \omega t - y_p \cos \omega t)}{(x_p^2 + y_p^2 + v_z^2 t^2)^{3/2}}.$$

Integrating over all time gives the radial displacement from one collision,

$$\Delta r = -2 \frac{ce}{B} y_p \left| \frac{\omega}{r_p v_z^2} \right| K_1 \left(\left| \frac{\omega r_p}{v_z} \right| \right), \tag{5}$$

where K_1 is the first modified Bessel function of the second kind. For a positron plasma in thermal equilibrium, Eq. (4) takes the form

$$D_r = \tfrac{1}{2} \int d^2 r_p dv_z f_e |v_z| \Delta r^2, \tag{6}$$

where $f_e(v_z) = (n/\sqrt{2\pi}\bar{v}) e^{-v_z^2/2\bar{v}^2}$ is the thermal equilibrium distribution at density n. Using this distribution with Eqs. (5) and (6) and integrating over the spatial variable θ, we obtain

$$D_r = 2\pi \int_{-\infty}^{\infty} dv_z \int_{r_{\min}}^{\infty} dr_p r_p \left(\frac{ce}{B}\right)^2 \frac{\omega^2}{|v_z|^3} K_1^2\left(\frac{\omega r_e}{|v_z|}\right) f_e. \quad (7)$$

The lower bound of the radial integral $r_{\min}$ is on the order of the atom radius r. Collisions occuring at smaller radii are no longer accurately modeled by unperturbed passing positron orbits, and are neglected in this drag calculation. The additive contribution to the energy loss rate from close collisions is estimated by Eq. (1).

If we let $r_{\min}=r$ and switch to scaled variables $s \equiv \omega r_p/\bar{v}$ and $x \equiv v_z/\bar{v}$,

$$D_r = \frac{1}{\sqrt{8\pi}} \left(\frac{c}{B}\right)^2 \frac{m_e \omega_p^2}{\bar{v}} \mathcal{F}(\xi) \quad (8)$$

with

$$\mathcal{F}(\xi) \equiv \int_{\xi}^{\infty} s\,ds \int_{-\infty}^{\infty} K_1^2\left(\frac{s}{|x|}\right) \frac{e^{-x^2/2}}{|x|^3} dx. \quad (9)$$

Here $\omega_p^2 = 4\pi e^2 n/m_e$ is the square of the positron plasma frequency and

$$\xi \equiv \frac{\omega r}{\bar{v}} = \frac{v_d}{\bar{v}} \quad (10)$$

is the "adiabaticity parameter." The function $\mathcal{F}(\xi)$ has the limiting forms

$$\mathcal{F}(\xi) \approx \ln^2 \xi \quad \text{for} \quad \xi \ll 1 \quad (11)$$

and

$$\mathcal{F}(\xi) \approx \sqrt{\frac{\pi^3}{6}}\, \xi^{-1/3} e^{-(3/2)(2\xi)^{2/3}} \quad \text{for} \quad \xi \gg 1. \quad (12)$$

Thus, as the positron drift speed ωr increases above the average thermal speed $\bar{v}$, the adiabatic cutoff manifests through a drop in the positron's diffusion coefficient.

To write the energy loss rate γ_{drag} in terms of the positron drift frequency, we use Eq. (3) and replace $v_d = \omega r$:

$$\gamma_{\text{drag}} = \frac{r}{\sqrt{8\pi}} \left(\frac{\omega r}{\bar{v}}\right)^2 \frac{\omega_p^2}{\bar{v}} \mathcal{F}\left(\frac{\omega r}{\bar{v}}\right).$$

For small bounce motion, the drift frequency ω can be expressed as

$$\omega \approx \frac{ec}{Br^3}.$$

Using this scaling, we can write an expression for γ_{drag} in terms of the adiabaticity parameter ξ:

$$\gamma_{\text{drag}} = \sqrt{2\pi\chi}\, n\bar{v} b^2\, \xi^{3/2} \mathcal{F}(\xi). \quad (13)$$

The energy loss rate is plotted in Fig. 2 (the solid line), and compared to the asymptotic forms (11) and (12) at large (dashed) and small (dotted) adiabaticity parameter ξ. While our form for γ_{drag} agrees with Ref. 4 for $\xi \ll 1$, our loss rate cuts off exponentially when $\xi \gtrsim 1$. Consequently, energy loss due to distant collisions becomes unimportant when $\xi > 1$.

Over a range of binding energies, collisional drag can be an important mechanism for relaxation to deeper binding in a guiding center atom. However, we have seen that the effect cuts off at a finite binding energy. To compare with the close collisions studied by Glinsky and O'Neil, we shift to scaled variables:

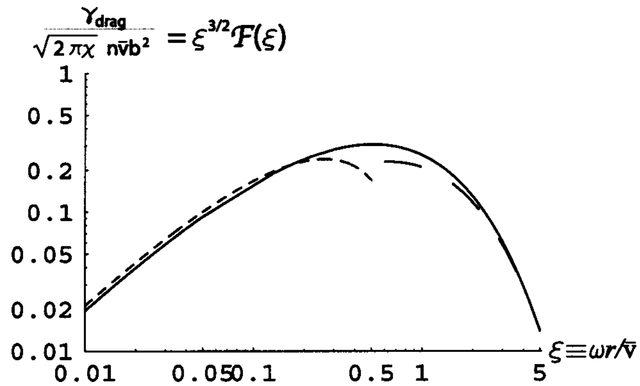

FIG. 2. The normalized recombination rate $\gamma_{\text{drag}}/\sqrt{2\pi\chi}n\bar{v}b^2 = \xi^{3/2}\mathcal{F}(\xi)$ due to distant collisions (solid line) plotted against the adiabaticity parameter $\xi = \omega r/\bar{v}$. We have assumed $\omega = ec/Br^3$. The limiting forms for $\xi \ll 1$ (dotted line) and $\xi \gg 1$ (dashed line) are also shown. The drop in γ at high ξ comprises the adiabatic cutoff.

$$\epsilon = U/k_B T,$$

$$\tau = t n \bar{v} b^2.$$

Using the small bounce motion scaling $\omega \approx ec/Br^3$, the adiabaticity parameter is given by

$$\xi = \frac{\omega r}{\bar{v}} \approx \epsilon^2 \chi.$$

Now we can write Eq. (13) in terms of χ and binding energy ϵ:

$$\hat{\gamma}_{\text{drag}} \equiv \frac{\gamma_{\text{drag}}}{n\bar{v}b^2} = \sqrt{2\pi}\,\epsilon^3 \chi^2 \mathcal{F}(\epsilon^2\chi). \quad (14)$$

From Eq. (1), the scaled energy loss rate due to close collisions is

$$\hat{\gamma}_{\text{close}} = \frac{1}{\epsilon^2}. \quad (15)$$

Figure 3 shows both energy loss rates. The drag is given for the parameters of the Athena ($B = 3\times 10^4$ G and $T = 15$ K$\Rightarrow \chi = 0.0257$) (Ref. 2) and ATRAP ($B = 5.4\times 10^4$ G and $T = 4.2$ K$\Rightarrow \chi = 2.11\times 10^{-3}$) (Ref. 1) experiments. At deep binding, energy loss due to drag mobility cuts off exponentially. Thus, short range collisions dominate at deep binding.

Both rates shown in the figure are calculated in the guiding-center-atom regime. When binding becomes very deep, the positron cyclotron motion becomes coupled to the orbital drift motion and the atom becomes chaotic. This occurs when

$$\omega \approx \Omega_c. \quad (16)$$

In the chaotic regime, the positron's motion can no longer be described by guiding center drift dynamics. Its motion is fast, enabling energy loss through radiation and a correspondingly

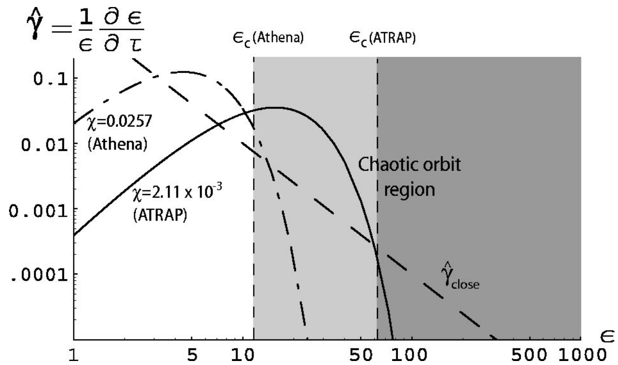

FIG. 3. The rate $\hat{\gamma}$ at which energy is lost from the bound charge system due to mobility drag (for Athena and ATRAP parameters); and for Glinsky–O'Neil small impact parameter collisions (dashed line). Drag dominates over a finite range in binding energy, depending on the factor χ.

fast transition to Kepler style orbits. We can write Eq. (16) in terms of the normalized binding energy ϵ and the parameter χ,

$$\frac{\omega}{\Omega_c} = \epsilon^3 \chi^2 = 1.$$

The approximate binding energy ϵ_c at which the atom becomes chaotic is given by

$$\epsilon_c = \chi^{-2/3}.$$

For the Athena parameters $\epsilon_c \approx 11.5$ and for ATRAP $\epsilon_c \approx 61$ (gray areas in Fig. 3). For these experiments, $\gamma_{\rm drag}$ cuts off close to where the positron orbit becomes chaotic.

The normalized time $\tau_{\rm relax}$ required for an atom to relax to the chaotic regime is given by

$$\tau_{\rm relax} = \int_1^{\chi^{-2/3}} \left(\frac{\partial \epsilon}{\partial \tau} \right)^{-1} d\epsilon, \tag{17}$$

where the total energy loss rate due to collisions is given approximately by adding the rates due to large impact parameter (drag) collisions and close (replacement) collisions:

$$\frac{\partial \epsilon}{\partial \tau} \approx \epsilon(\hat{\gamma}_{\rm drag} + \hat{\gamma}_{\rm close}).$$

Table I shows the relaxation time $\tau_{\rm relax}$ compared to the estimated time $\tau_{\rm esc}$ that a bound pair takes to escape the positron cloud for the Athena and ATRAP parameters. Each time is normalized by the collision frequency $n\bar{v}b^2$, estimated from Refs. 1 and 2. For ATRAP, antiprotons were assumed to be at 10 meV. For Athena, the antiprotons were assumed thermal (15 K). The escape time $\tau_{\rm esc}$ was estimated as the transit time for an atom traveling at the antiproton velocity to reach the plasma edge. For Athena, escape paths

TABLE I. The normalized time (number of collision times) $\tau_{\rm relax}$ required for a guiding-center atom to collisionally relax to the chaotic orbit regime (see text). Bound pairs escape the positron cloud in approximately $\tau_{\rm esc}$ collision times. $\perp$ and $\parallel$ refer to escape transverse and parallel to **B**, respectively.

	Athena		ATRAP
χ	0.0257		2.11×10^{-3}
$\tau_{\rm relax}$	≈ 390		≈ 18
$\tau_{\rm esc}$	$\perp \approx 40$	$\parallel \approx 250$	$\parallel \approx 1.5$

both transverse to the field, a maximum distance of roughly 0.5 cm, and parallel to the field, a maximum distance of 3 cm, were considered. Atoms escaping parallel to **B** would remain in the plasma longer, evolving to deeper binding. For ATRAP, the path was chosen on axis, a maximum distance of 0.1 cm. These estimates indicate that, on average, guiding-center atoms remain in the plasma about one-tenth to one-half the length of time required to relax to the chaotic regime. More accurate calculations are currently underway.

Figure 3 shows that small impact parameter collisions dominate at very shallow and at very deep binding, but that long range collisions can be important at intermediate binding energies. However, note that the precise location of the adiabatic cutoff in Fig. 3 depends on our choice for $r_{\rm min}$ in Eq. (7). We assumed $r_{\rm min} = r$, but taking $r_{\rm min}$ larger would move the cutoff to lower energy, further reducing the effect of long-range collisions. Also, a Vlasov wake calculation to be presented in a future paper suggests an even steeper functional form for the adiabatic cutoff. While the existence of an adiabatic cutoff at $\xi \approx 1$ is incontestable, its precise form and location are not known. To fully answer this important question, one must consider short and medium range collisions with a computer simulation and graft that result onto our drag calculation. This work is currently underway.

ACKNOWLEDGMENTS

The authors thank Professor C. F. Driscoll and Professor T. M. O'Neil for useful discussions.

This work was supported by the National Science Foundation Grant No. PHY-9876999 and the Office of Naval Research Grant No. N00014-96-1-0239.

[1] G. Gabrielse, N. S. Bowden, P. Oxley *et al.*, Phys. Rev. Lett. **89**, 213401 (2002).
[2] M. Amoretti, C. Amsler, G. Bonomi *et al.*, Nature (London) **419**, 456 (2002).
[3] M. E. Glinsky and T. M. O'Neil, Phys. Fluids B **3**, 1279 (1991).
[4] L. I. Men'shikov and P. O. Fedichev, JETP **81**, 78 (1995).
[5] P. O. Fedichev, Phys. Lett. A **226**, 289 (1997).
[6] F. Reif, *Fundamentals of Statistical and Thermal Physics* (McGraw–Hill, New York, 1965), p. 567.